The shading zone problem in geodesic voting and its solutions for the segmentation of tree structures. Application to the segmentation of Microglia extensions

Youssef Rouchdy[1,2]
University of Pennsylvania[1]
3600 Market Street, Philadelphia, PA, USA
Youssef.Rouchdy@uphs.upenn.edu

Laurent D. Cohen[2]
CEREMADE, Université Paris Dauphine[2]
75775 PARIS CEDEX 16 - FRANCE
cohen@ceremade.dauphine.fr

Abstract

This paper presents a new method to segment thin tree structures, which are for example present in microglia extensions and cardiac or cerebral blood vessels. The minimal path method allows the segmentation of tubular structures between two points chosen by the user. A feature potential function is defined on the image domain. This corresponds to geodesic paths relatively to the metric weigthed by the potential. We propose here to compute geodesics from a set of end points scattered in the image to a given source point. The target structure corresponds to image points with a high geodesic density. The geodesic density is defined at each pixel of the image as the number of geodesics that pass over this pixel. Since the potential takes low values on the tree structure, geodesics will locate preferably on this structure and thus the geodesic density should be high. The segmentation results depend on the distribution of the end points in the image. When only the image border is used to perform geodesic voting, the obtained geodesic density is contrasted and easy to use for image segmentation. However, when the tree to segment is complex a shading problem appears: some contours of the image can have a null density since geodesic have a better way around this region. To deal with this problem we propose several different strategies: we use several source points for the propagation by Fast Marching; a set of characteristic points or an adaptive set of points in the image or make successive segmentation in the shading zones. Numerical results on synthetic and microscopic images are presented.

1. Introduction

We are interested in the segmentation of tree structures like those appearing in medical images (vascular tree) or biological images (extensions of microglia). Although our aim was initially to extract microglia from confocal microscopy images, the methods we introduce are generic and can be used for any type of tree structure. A simple use of the image intensities is not sufficient to extract directly a tree structure. Malladi et al. [8] used the Level Set methods to extract information from MRI data (which present approximately the same difficulties as the confocal microscope images). Although much work is devoted to the segmentation of vascular tree, few attempts have been made to extract microglia extensions and these attempts were restricted to the main branches ([5], [15]). From our experience with vascular tree segmentation, we can tell that microglia segmentation can be much more difficult, due to very thin parts and noise. Also, the segmentation of vascular tree is usually obtained using a priori information. For example many approaches need to give a point for each branch. The Fast Marching method, introduced by Sethian in [12], and adapted by Cohen et al. [2] to extract tree structures, demands less computation time than the Level Set method and works with only one point chosen by the user on the tree. However, this method depends on *a priori* information about the target. In our case no *a priori* information about the tree structure is available. We propose in this paper geodesic voting strategies for the segmentation of tree structures. These methods consist in extracting a large number of geodesics from the image. The target corresponds to the image points with high geodesic density. The original approach of geodesic voting was proposed in [10]. These method allowed the extraction of tree structure from only one point given by the user. However, the method had a limitation that we call shading zone. In this paper we point out this problem and propose different solutions to fix it. In section 2, tools used to extract minimal paths with the Fast Marching algorithm are presented. In sections 3 and 4 the geodesic voting method is introduced and geodesic voting methods to deal with shading zones problem were proposed. Finally, in section 4.4 discussion and segmentation results

are presented.

2. Background

2.1. Minimal paths

The minimal path theory for the extraction of contours from the image was inspired by the principle of Fermat: the light trajectory minimizes the optical distance between $x_0 = y(0)$ and $x = y(t)$, e.g. it gives the curve y that minimizes the distance

$$\tau(x_0, x) = \int_{t_0}^{t} \frac{\mathrm{d}s}{c\big(y(s)\big)} \tag{1}$$

where propagation speed c is a function depending on the medium of the propagation. In homogenous media the function c is a constant, the trajectories correspond to lines. In a medium with two regions, the function c takes two values: c_1 in the first region and c_2 in the second region. The trajectory, in this case, corresponds usually to two joint segments, each segment belonging to one region. We are interested here in the case of a medium with a continuous velocity c, see [3].

In the context of image segmentation Cohen and Kimmel proposed, in [3], a deformable model based on the optical distance (1). The model is formulated as a calculus of variation problem :

$$\text{Min} \int_0^t \big(w + P(y(s))\big)\mathrm{d}s, \tag{2}$$

the minimum is considered in

$$\big\{y \ : [0,t] \longrightarrow \mathbb{R}^2 : \quad y(0) = x_0, \quad y(t) = x\big\}.$$

The constant w imposes regularity on the curve. $P > 0$ is a potential computed from the image, it takes lower values near the edges or the features. For instance

$$P(y(s)) = I(y(s)), \quad P(y(s)) = g(||\nabla I||),$$

where I is the image and g is a decreasing function.

To compute the solution associated to the source x_0 of this problem, we consider a Hamiltonian approach: Find the travel time U that solves the eikonal equation

$$||\nabla \mathrm{U}(x)|| \quad = \quad w + P(x) \quad x \in \Omega \tag{3}$$

The ray y is subsequently computed by back-propagation from x by solving the ODE

$$y'(s) = -\nabla \mathrm{U}(y). \tag{4}$$

The only stable schemes that solve the eikonal equation compute a viscosity solution [4]. The first work that uses the viscosity solution is from Vidale [14]. Based on this work Fatemi et al. [6] proposed the first numerical scheme to solve the eikonal equation. To solve eikonal equation through iterations [11], at least $O(mn^2)$ are needed, where n is the total number of grid points and m is the number of iterations that permit an estimation of the solution. In the next section, we present the Fast Marching algorithm introduced in [12] to solve this problem in complexity $O\big(n\log(n)\big)$.

2.2. Fast Marching method

The idea behind the Fast Marching algorithm is to propagate the wave in only one direction, starting with the smaller values of the action map U and progressing to the larger values using the upwind property of the scheme. Therefore, the Fast Marching method permits only one pass on the image starting from the sources in the downwind direction. Here, the principle of the Fast Marching method is given, for details see [12, 13, 1]. The grid points are partitioned into three dynamic sets: trial points, alive points and far points. The trial points correspond to a dynamic boundary that separates far points and alive points. At each step, the trial point with the minimum value of the action map U is moved to the set of alive points, which are the grid points for which a value U has been computed. The values of alive points do not change. To reduce the computing time, the trial points are stocked in a data structure referred to as min-heap (the construction of this data structure is described in [12, 13]). The complexity to change the value of one element of the min-heap is $O\big(n\big)$. Hence, the total work for Fast Marching is $O\big(n\log(n)\big)$. The Dijkstra algorithm, which is also used to find a minimal path, has the same complexity as the Fast Marching algorithm. However, the Dijkstra algorithm gives a linear approximation and there is no uniqueness result contrary to the Fast Marching algorithm, which converges toward the unique viscosity solution.

3. Segmentation by geodesic voting of tree structures

With the Fast Marching method we can extract the minimal path between two points. Here, the aim is to extract a tree with just one point chosen by the user. When *a priori* information is available about the length of the contour that one wants to extract, Cohen and al. proposed in [2] a method to extract a tree structure from one point selected by the user. In the following sections, a method is proposed for the segmentation of tree structures from only one given point without having any *a priori* information about the tree to extract. The method uses a new concept for the image segmentation. The method consists in computing geodesic curves from a st of image points. The tree structure corresponds to the points with high geodesic density. First we

choose the root of the tree structure and we propagate a front in the whole image with the Fast Marching method. Then, the geodesic paths from a set of points, denoted by $\{x_k\}_{k=1}^N$, is extracted by solving the ODEs:

$$\frac{\partial y_k}{\partial s} = -\nabla \mathrm{U}\big(y(s)\big),\ y_k(0) = x_k,\ k = 1, \cdots, N \qquad (5)$$

The set of points $\{x_k\}_{k=1}^N$ can be the boundary of the image domain. We define the voting score or the geodesic density at each point p of the image by

$$\mu(p) = \sum_{k=1}^{N} \delta_p(y_k) \qquad (6)$$

the function $\delta_p(y)$ returns 1 if the path y crosses the pixel p, else 0. As we can see in figure 1 the geodesic paths converge on the tree structure, giving it a high density value. In this example the potential P used to propagate by Fast Marching method is the image. Note that a simple thresholding can be used to extract efficiently the tree structure. The threshhold can be automatized for a class of images. For example we have used the same threshhold to segment Microglia images. For other classes of images the threshold could be easily reset manually by testing the method on a few images.

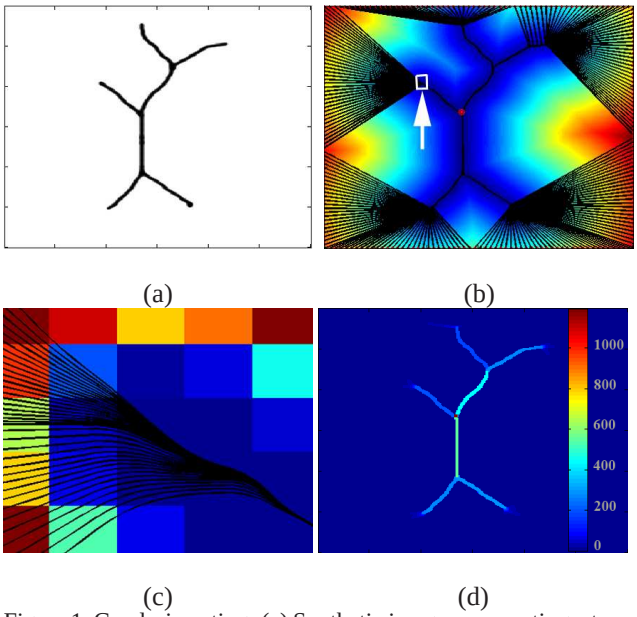

Figure 1. Geodesic voting. (a) Synthetic image representing a tree; (b) extraction of geodesics. The red circle represents the source point from which the propagation is started and black lines represent paths extracted from the image border to the source point. The paths are superimposed on the distance map. (c) zoom on the square indicated by an arrow in figure (b). (d) geodesic density computed from (b). The geodesic density of each pixel in the image corresponds to the number of trajectories crossing the given pixel.

4. Solutions for shading zones problem

The segmentation by geodesic voting method uses only the image boundary, which has the advantage that the score map is contrasted, which facilitates the segmentation of the tree structure. However, for complex tree structures the image border is not sufficient for segmentation, see figure 2. Indeed, the minimal paths pass through points that realize a balance between minimizing the paths length and following the paths where the values of the potential are as small as possible. Therefore, some zones had a null score -e.g. they had no geodesic density- although they contained leafs of the tree as we can see in the figure 2-Right. We call the regions with null values of the score map, *shading zones* and the segmentation problem related to these regions a *shading zones problem*. In the following sections, different strategies to deal with shading zones problem are presented.

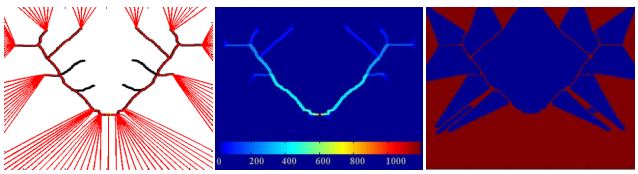

Figure 2. Shading zones. Left panel: extraction of geodesics. The red circle represent the source point from which the propagation is started and the red lines represent paths extracted from the image border to the source point. The paths are superimposed on the image; only 10 per 100 of the paths extracted are shown in the figure. Center panel: geodesic density. Right panel: shading zones. The blue regions correspond to the extracted shading zones; these are zones without vote.

4.1. Multi-propagation

We observed that changing the source point in the tree structure can partially solve shading problems. In the figure 3-c we took two different source points s_1 on the leaf f_1 and s_2 on the leaf f_2. With the source point s_1 it was possible to extract the leaf f_1 from the score map $\mathcal{S}_1$ but not the leaf f_2, whereas with the source point s_2 it was possible to extract the leaf f_2 but not the f_1, see figures 3-a-b-d-e. We remark that the sum of the two score maps $\mathcal{S}_1$ and $\mathcal{S}_2$ allowed to segment both leafs. Hence, we propose to compute for each junction and for each extremity of the tree structure the associated score map. Subsequently, we define the *global score map* as sum of all score maps. Furthermore, the junctions and the extremities of the tree correspond to the corner points, see figures 3-c-f. To detect corner points, the detector of Harris points is used [7]. The global score map is defined by:

$$\mu = \sum_{i=1}^{N} \mathcal{S}_i. \qquad (7)$$

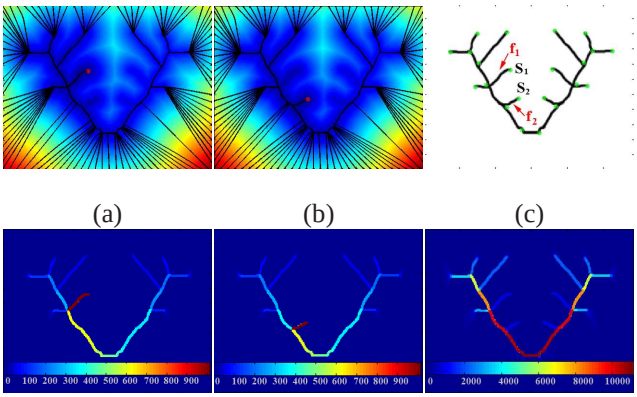

Figure 3. Voting by multi-propagation. (a) and (b): red circles represent the source point from which the propagation is started, the blue lines represent paths extracted from the image border to the source point, the paths are superimposed on the image. Only 10 per 100 of the paths extracted are shown in the figures; (c) The green circles correspond to Harris points used to run multi-propagation superimposed to the image. (d) and (e) are respectively the score map associated respectively to the geodesics map (a) and (b). (f) corresponds to the global distance map computed by multi-propagation.

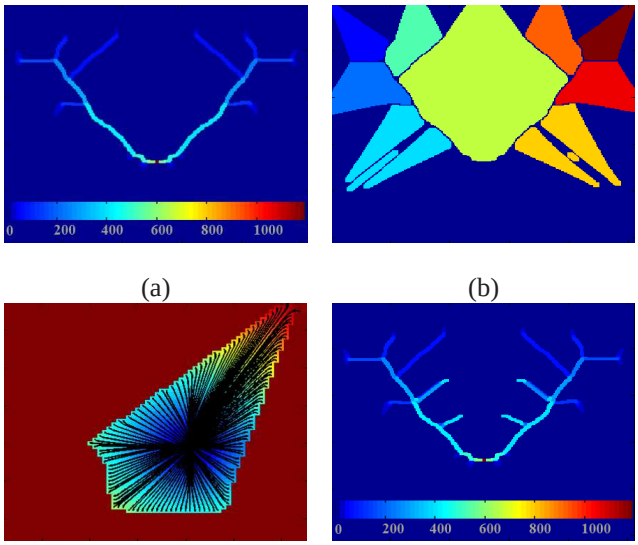

Figure 4. Successive geodesic voting. (a) score map computed from the image border; (b) labeling of the extracted shading zones, 14 shading zones were detected; (c) extraction of geodesic paths from a shading zone; (d) score map obtained by applying geodesic voting to the shading zones.

where N is the number of the Harris points detected and $\mathcal{S}_i$ is the score map associated to the Harris point h_i.

Note that the use of the Harris points instead of all image points to compute the global map reduces considerably the computing time.

4.2. Successive geodesic voting

Here, we propose to use a successive segmentation to solve the problem of shading zones. First, we chose a point to initialize the propagation on the tree structure. From the distance map associated to the initial point the score map is computed, see figure 4-a. Subsequently, the shading zones are extracted from the score map and labeled, see figure 4-b. For each shading zone we run a geodesic voting from the border of the shading zone, see figure 4-c. The final score map is computed as a sum of all score maps computed from the initial image and from the shading zones, see figure 4-d.

4.3. Adaptive voting

In this section, we present another approach to deal with shading zone problems using only one source point. This method consists in extracting minimal paths from the border and inside the image to compute a score map. One can use the whole image to extract a path, however this method is expensive in computing time. In this section we propose to use an anisotropic meshing of the image points to run the geodesic voting. The mesh is dense on the tree structure and sparse outside. Hence, the score map is very contrasted, allowing a good segmentation of the tree structure. The method used to built automatically such anisotropic meshing is based on a Voronoi diagram construction and the Fast Marching propagation, [9].

In the following, we describe how this method works. Firstly, we have a point s_1 with an associated distance map computed with the Fast Marching method. Let us assume that a set of points $S_n = \{s_1, \cdots, s_n\}$ and their associated distance map U are computed. We construct then the set $S_{n+1} = \{s_{n+1}\} \cup S_n$, where s_{n+1} is the farthest point of the image from the set S_n. The distance map U_{n+1} is defined by the relation $\mathrm{U}_{n+1} = \min\left(\mathrm{U}_n, \mathrm{U}_{s_{n+1}}\right)$, where $\mathrm{U}_{s_{n+1}}$ is the distance map computed from s_{n+1}. The distribution of the points on the image with farthest points process is stopped when the desired number of points is reached.

The farthest points added at each iteration correspond to the maximal values of the geodesic distance. Therefore, the resulting meshing is dense in regions with smaller value for the propagation speed $\mathcal{F}$, and sparse in regions with higher values of $\mathcal{F}$. The speed function is computed as the inverse of the potential P defined in section 2.1. The speed function $\mathcal{F} > 0$ computed from the image take the smallest values on the tree structure and the largest outside. Therefore, the meshing is dense on the tree structure and sparse outside, see figures 5-Left-Center. Hence, the score map is contrasted and allows an easier segmentation of the tree structure, see figure 5-Right.

Note that we can applied a multi-propagation method to

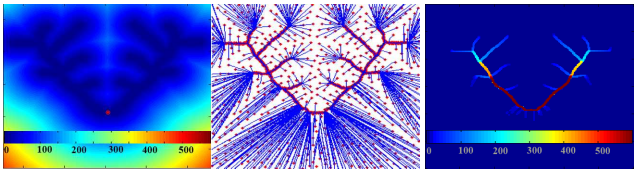

Figure 5. Adaptive voting. Left panel: distance map used to extract geodesics from the farthest points. Center panel: extraction of geodesics; the red circle represents the source point and the blue lines correspond to the geodesics extracted from the farthest points to the source points. Right panel: computed geodesic density.

Voting method	Computing time	Contrast
Border, sect. 3	27.08 sec.	4
Multi, sect. 4.1	481.78 sec.	1
Adaptive, sect. 4.3	94.94 sec.	2
Successive, sect. 4.2	63.01 sec.	3

Table 1. Computing time and classification of the five proposed geodesic voting methods for a 220×300 pixel image.

anisotropic meshing as presented for Harris points in section 4.1.

4.4. Discussions and results

In sections 3 and 4, we have proposed geodesic voting methods to extract tree structures from only one point given by the user without using *a priori* information, in contrast to [2] which uses information about the length of the tree to extract. The problem of shading zones was pointed out and treated to complete the segmentation results in section 4. The segmentation by geodesic voting from the border gives a contrasted geodesic density and demands less computing time. However, there is the problem of shading zones as we have explained in section 4. Table 1, compares the proposed methods according to the computing time and the quality of the computed geodesic density. The column "Contrast" gives the classifications of the five methods (1 is for best).

Regarding the computing time and the quality of the geodesic density, we have chosen to use adaptive voting, presented in section 4.3, to segment microglia extensions from confocal microscope images. Figure 6 shows the segmentation results obtained with this method. Note that the density maps shown in figure 6-(right column) are not thresholded. The numerical results obtained with this method were very satisfying in terms of rapidity of analysis and coherence with the visual aspect of the cells. Although this method needs to be compared to manual segmentation, the present results are encouraging and should lead to a future extension of the method to 3D segmentation.

In conclusion, this work shows that the proposed geodesic voting methods can be used to segment tree structures in images. The major contributions of this paper are: we have pointed out the shading zone problem related to the segmentation with geodesic voting, and we have proposed adequate solutions to solve this problem. We have applied this method to the segmentation of microglia images which are very noisy. The proposed methods are generic, and can be used to extract any type of tree structure.

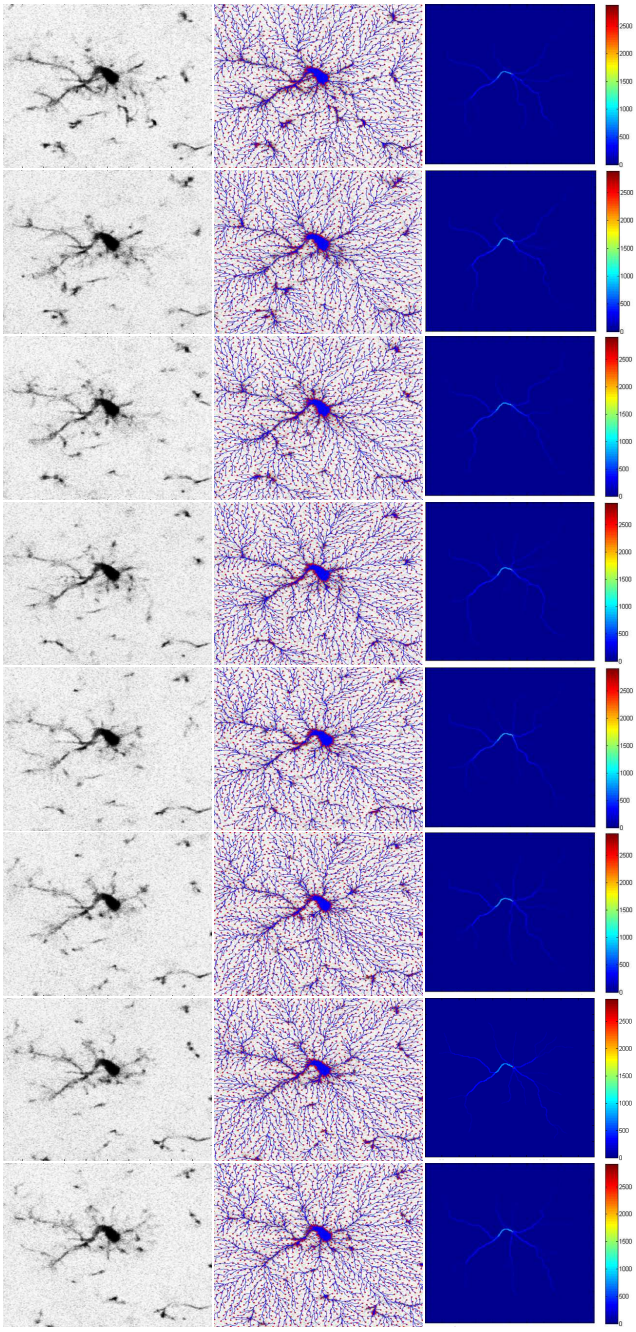

Figure 6. Results. Left column: Microglia images. Center column: extraction of geodesics; the red circle represents the source point and the blue lines correspond to the geodesics extracted from the farthest points to the source points. Right column: computed geodesic density.

References

[1] L. Cohen. Minimal paths and fast marching methods for image analysis. In *Handbook of mathematical models in computer vision*, pages 97–111. Springer, New York, 2006. 2

[2] L. D. Cohen and T. Deschamps. Segmentation of 3D tubular objects with adaptive front propagation and minimal tree extraction for 3D medical imaging. *Math. Models Methods Appl. Sci.*, 10(4):289–305, 2007. 1, 2, 5

[3] L. D. Cohen and R. Kimmel. Global minimum for active contour models: A minimal path approach. *International Journal of Computer Vision*, 24(1):57–78, 1997. 2

[4] M. G. Crandall and P.-L. Lions. Viscosity solutions of Hamilton-Jacobi equations. *Trans. Amer. Math. Soc.*, 277(1):1–42, 1983. 2

[5] D. D. et al. Atp mediates rapid microglial response to local brain injury in vivo. *Nature Neuroscience*, 8(6):752–758, 2005. 1

[6] E. Fatemi, B. Engquist, and S. Osher. Numerical solution of the high frequency asymptotic expansion for the scalar wave equation. *J. Comput. Phys.*, 120(1):145–155, 1995. 2

[7] C. Harris and M. Stephens. A combined corner and edge detection. In *Proceedings of The Fourth Alvey Vision Conference*, pages 147–151, 1988. 3

[8] R. Malladi and J. Sethian. Level set methods for curvature flow, image enchancement, and shape recovery in medical images, 1997. 1

[9] G. Peyré and L. D. Cohen. Geodesic remeshing using front propagation. *Int. J. Comput. Vision*, 69(1):145–156, 2006. 4

[10] Y. Rouchdy and L. D. Cohen. Image segmentation by geodesic voting. application to the extraction of tree structures from confocal microscope images. In *The 19th International Conference on Pattern Recognition*, Tampa, Florida, 2008. 1

[11] E. Rouy. Numerical approximation of viscosity solutions of first-order Hamilton-Jacobi equations with Neumann type boundary conditions. *Math. Models Methods Appl. Sci.*, 2(3):357–374, 1992. 2

[12] J. Sethian. A fast marching level set method for monotonically advancing fronts. In *Proc. Nat. Acad. Sci.*, volume 93, pages 1591–1595, 1996. 1, 2

[13] J. A. Sethian. *Level set methods and fast marching methods*, volume 3 of *Cambridge Monographs on Applied and Computational Mathematics*. Cambridge University Press, Cambridge, second edition, 1999. 2

[14] J. Vidale. Finite-difference calculation of traveltime. *B. Seismol. Soc. Am.*, 78:2062–2076, 1988. 2

[15] L.-J. Wu and M. Zhuo. Resting microglial motility is independent of synaptic plasticity in mammalian brain. *J. Neurophysiol*, 99:2026–2032, 2008. 1